

## Severe plastic deformation processes for thin samples

R. Lapovok · A. Pougis · V. Lemiale · D. Orlov ·  
L. S. Toth · Y. Estrin

Received: 5 February 2010/Accepted: 9 March 2010/Published online: 27 March 2010  
© Springer Science+Business Media, LLC 2010

**Abstract** Among the known severe plastic deformation (SPD) techniques, one particular group can be defined as SPD processing of thin samples. Their distinctive feature is that one of the sample dimensions, namely the thickness, is much smaller than the other two dimensions. Examples include High Pressure Torsion and two recently developed techniques: the Cone–Cone Method and the High Pressure Tube Twisting. The mentioned group of SPD processes involve frictional forces acting on the large surfaces and a high hydrostatic pressure within the deformation zone. These techniques are particularly suited for microforming of metals. In this article, we outline the commonalities between these three techniques. The microstructure of copper samples deformed by all the three processes is presented and compared with those obtained by equal-channel angular pressing as a reference bulk forming SPD technique.

### Introduction

Severe plastic deformation (SPD) techniques have recently advanced to main processing routes to enable rapid grain refinement in metals leading to ultrafine grained (UFG) microstructures [1]. Among the known SPD techniques used to produce bulk UFG materials, one group can be defined as SPD processing of thin samples or work-pieces. Their distinctive feature is that one of the sample dimensions, namely the thickness, is much smaller than the other two dimensions. The well-known process of High Pressure Torsion (HPT) [2] applied to a specimen whose thickness is much smaller than the diameter, as well as the less-known Cone–Cone Method (CCM) [3, 4] and the High Pressure Tube Twisting (HPTT) [5] process applied to thin conical or tubular samples are all in this category of SPD techniques.

For all of them, a severe shear strain is imposed within the thickness of the sample due to the difference in magnitude of the material flow velocities at two large surfaces, rather than by a change in the velocity direction (as is the case, e.g. for equal-channel angular pressing). The mentioned group of SPD processes involve friction forces acting on the large surfaces and a high hydrostatic pressure within the deformation zone. It should be noted that scale-up of such processes relying on friction will be almost impossible compared to other SPD techniques, such as equal-channel angular pressing or twist extrusion. However, these techniques may find their place in future manufacturing as novel microforming operations [6].

In this article, the commonalities between HPT, CCM and HPTT are outlined. The microstructure of copper samples deformed by all the three techniques are reported and discussed vis-à-vis microstructures produced by the most popular bulk forming SPD technique, viz. equal-channel angular pressing.

R. Lapovok (✉) · D. Orlov · Y. Estrin  
ARC Centre of Excellence for Design in Light Metals,  
Department of Materials Engineering, Monash University,  
Clayton, VIC, Australia  
e-mail: ramma.lapovok@spme.monash.edu.au

A. Pougis · V. Lemiale · Y. Estrin  
Division of Process Science and Engineering, CSIRO, Clayton,  
VIC, Australia

L. S. Toth  
Laboratoire de Physique et Mécanique des Matériaux,  
Université Paul Verlaine-Metz, Ile du Saulcy,  
57045 Metz, France

## Experimental methods

All experiments were performed on commercial purity copper with the average grain size of 20  $\mu\text{m}$ , annealed at 600°C for 2 h.

The HPT experiments were made on samples of 1 mm thickness and 4 mm radius (Fig. 1a) using three levels of pressure: 1.0, 1.5 and 1.9 GPa. The HPT samples were deformed by five turns with a speed of rotation of 1 rpm.

The CCM experiments involved conical specimens 0.4 mm in thickness, Fig. 1b, and the same levels of normal pressure on the specimen walls. CCM samples were deformed up to 10 turns with a speed of rotation equal to 2 rpm.

Finally, the copper tubes subjected to HPTT process had the outer diameter of 10 mm and the wall thickness of 1 mm, Fig. 1c.

Deformation by all the three SPD processing methods was performed using an accessory unit attached to a moving table of an Instron 4505 testing machine, Fig. 2. The motor (1) used to drive the accessory unit is a high torque AC electric motor controlled by a Programmable Logic Controller (PLC). The torque of the motor is increased by a 50:1 reduction gearbox, whose output has a die drive (2) attached to it. The PLC allows the rotational speed of the motor to vary between 2 and 50° sec<sup>-1</sup> and the torque to take values up to 500 Nm. The die (3) is fixed in the gear box drive, while the punch (4) is mounted on the plate attached to the stationary table of Instron, which is in contact with a loading cell (5) controlling the required compression force on the sample during deformation.

The microstructures produced by the three SPD techniques employed were investigated by optical microscopy (OM). HPTT specimens were also studied by scanning electron microscopy (SEM). In all the cases, sections through the specimen thickness were inspected. In all the three kinds of SPD process, the resulting microstructures were compared after five turns, which corresponds to a typical equivalent strain within the wall of HPTT and CCM specimens (or at the periphery of HPT specimens) of the order of 70, cf. the respective expressions for the equivalent strain below.

**Fig. 1** Copper samples used for **a** HPT; **b** CCM processing; and **c** HPTT processing

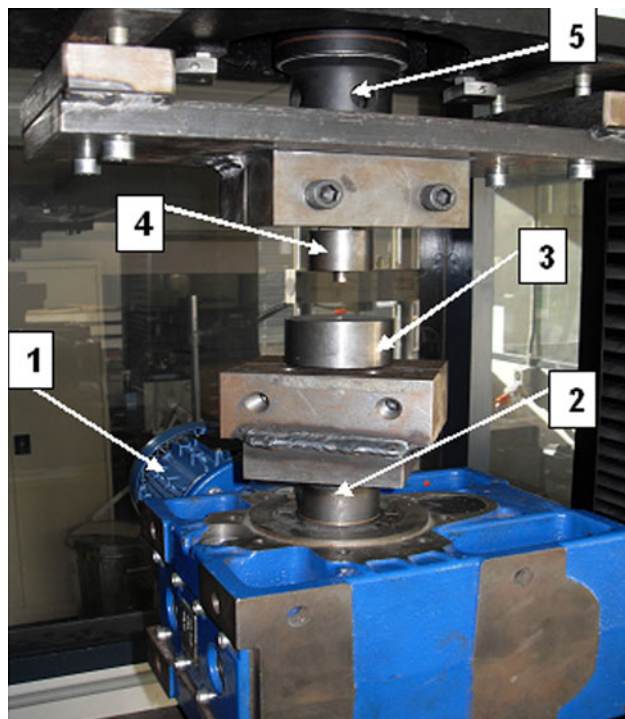
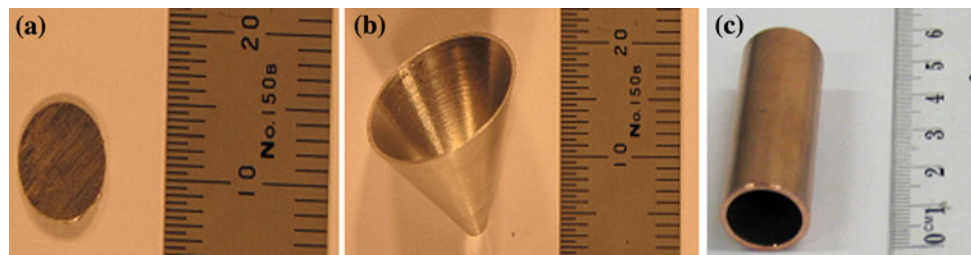


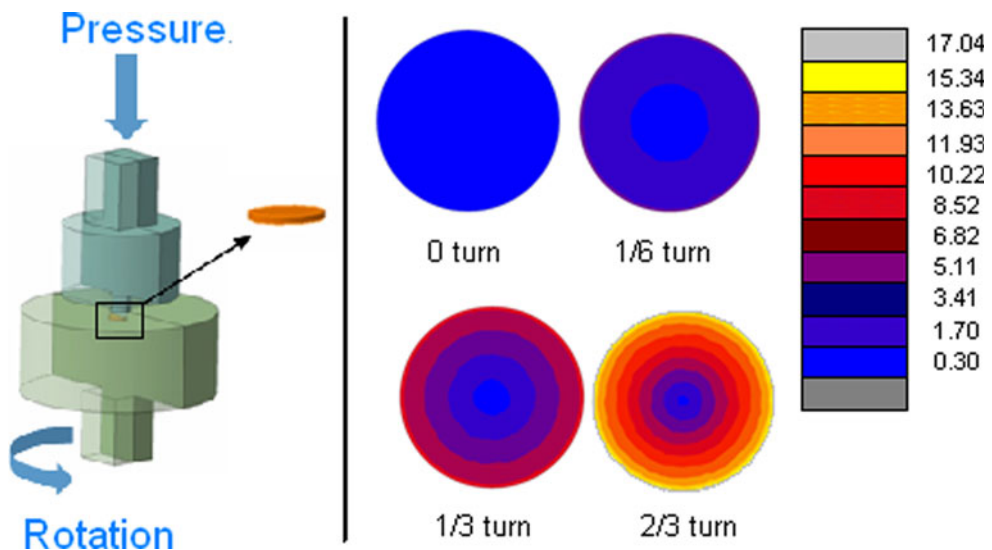
**Fig. 2** Assembly of the accessory unit on an Instron testing machine with an HPT die

## High pressure torsion

The high pressure on the punch and the presence of a small gap between punch and HPT die led to a thin ribbon of metal (about 370  $\mu\text{m}$  of thickness) extruding backward through the gap during the deformation. As a result, the thickness of the sample decreased from the initial 1 mm to final 0.8 mm for a pressure of 2 GPa on the top surface of the HPT specimen.

The HPT process was simulated using the finite element (FE) package MARC. Computations were carried out in two stages: first, the compression by the punch to 2 GPa, and second, rotation under compression at a fixed level of pressure (2 GPa). The model of the process and evolution of equivalent strain distribution in the sample with the number of revolutions are shown in Fig. 3. It can be seen that a pronounced strain gradient exists in the sample

**Fig. 3** FE model of HPT and the evolution of the distribution of the equivalent strain in the sample with the amount of tool rotation



within the first turn and, as shown in [7], at least eight turns are required to approach uniformity of strain across the sample. (Of course, due to the geometry of the HPT process, shear strain cannot assume non-zero values at the rotation axis, cf. Eq. 1.)

The analytical formula for the equivalent (von Mises) strain at the periphery of an HPT specimen associated with shear deformation,

$$\varepsilon_{\text{eq}} = \frac{2\pi N \cdot r}{\sqrt{3} \cdot t}, \quad (1)$$

where  $N$  is the number of turns, and  $r$  and  $t$  are the distance from the rotation axis and the thickness of the sample, respectively, gives the values of the equivalent strain at a distance from the centre of the sample specified as  $r = 0.8R$  (3.02 for 1/6 turn; 6.04 for 1/3 turn and 12.09 for 2/3 turn). Here,  $R$  denotes the specimen radius.

In contrast with the uniformity of strain distribution after two turns predicted by the model, the microstructure of the

experimental samples was non-uniform even after five turns, Fig. 4. The layers of copper close to the contact surfaces with the die and the punch consisted of highly twisted grains. The thickness of these layers in the centre of the samples was quite small, about 17 µm, Fig. 4a. Between these two layers, the microstructure consisted of very fine grains, which are difficult to resolve by optical microscopy (OM). Closer to the edges, where the material was extruded into the gap between the specimen and the tooling, twisted grains were visible in the mid-part of the sample, Fig. 4b. Near the edge next to the extrusion gap, the thickness of the layer with twisted grains increased to about 30 µm, Fig. 4c.

#### The cone-cone method

In this process described in Refs. [3, 4], thin-walled cone-shaped samples with a radius of 10 mm in the cone base

**Fig. 4** Optical microscopy images of a sample deformed by five turns of HPT  
a microstructure in the centre of the sample; b microstructure at the edge of the sample (the part extruded in the gap can be seen in the top right corner); and c microstructure at the edge of the sample next to the gap

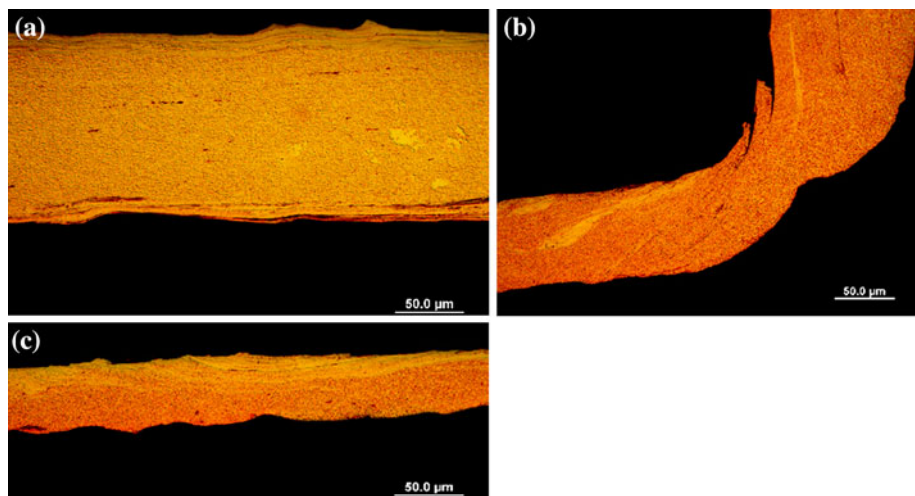
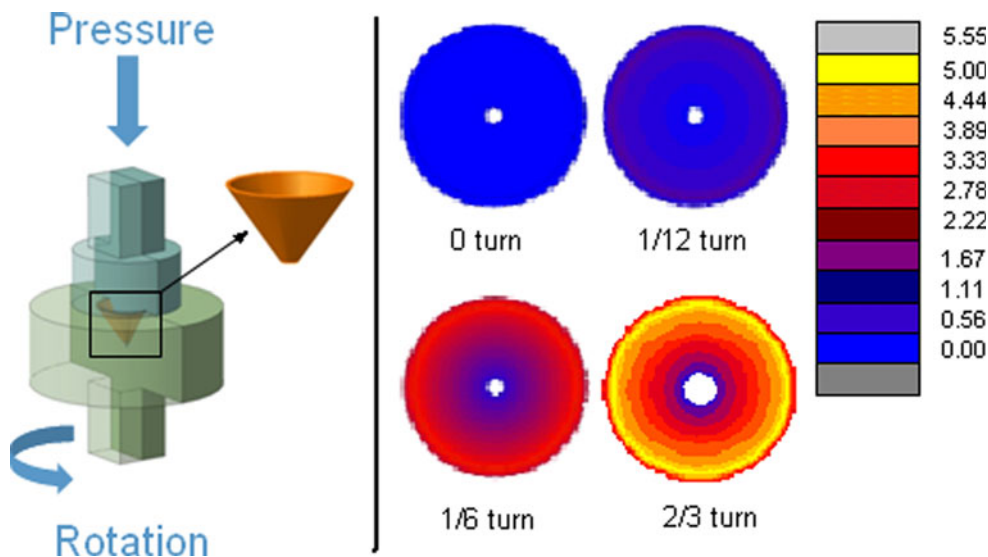


**Fig. 5** FE model of the CCM process (*left*) and the evolution of the equivalent strain distribution in the sample with the degree of rotation of the punch



and a height of 15 mm were deformed by up to five turns. A large number of turns were required to reduce non-homogeneity of strain similar to that occurring under HPT. An FE model of the process and the evolution of the equivalent strain distribution in a sample with the increasing degree of rotation of the punch are shown in Fig. 5. It can be seen that strain decreases towards the apex of the cone linearly with the distance along the central axis.

The analytical expression defining the equivalent plastic strain in the conical sample [3],

$$\varepsilon_{\text{eq}} = \frac{2\pi N \cdot R(x)}{\sqrt{3} \cdot t}, \quad (2)$$

also shows non-homogeneity of strain inherent in the geometry of the process. Here,  $N$  is the number of turns of the ram,  $t$  is the thickness of the sample and  $R(x)$  is the (external) radius of a circular cross-section normal to the cone axis at a distance  $x$  from the apex.

In order to assess the homogeneity of the microstructure, optical microscopy of samples subjected to five turns was carried out. Unlike the FE simulation (using the MARC software) for this condition, which predicts nearly homogeneous strain distribution, the OM images of the area close to the cone base (edge of the ‘funnel’) show that microstructure, Fig. 6a, was not refined uniformly, as distinct from the pretty homogeneous microstructure in the middle section of the cone, Fig. 6b. Indeed, while the microstructure in the middle section is characterised by a uniform distribution of very fine grains, which are difficult to resolve by optical microscopy, large grains with twins can still be seen in the edge region.

This observation can be explained by a variation of the normal stress along the contact surfaces between the sample and the tooling. In the present case, this is caused by the fact that the deforming body has a free edge and

unconstrained plastic flow along the lateral surface of the cone occurs. Similar to the upsetting process, the normal pressure has a maximum in the middle region and drops towards the free surfaces. Therefore, friction in this region is also lower, which allows slipping of the conical sample relative to the die and/or the punch leading to a significant reduction of strain in the region close to the sample edge.

### High pressure tube twisting

In this process, a tube sample with diameter of 10 mm and wall thickness of 1 mm is pressed against a rotating die by the pressure created by elastic deformation of a compressed mandrel. We should distinguish here the difference between the HPTT process described in [5] and HPTT process used in this study. In contrast to the design with completely confined samples [5], here the edges of a sample were not confined and the material could flow to the free surface at the edges of a tube. This made it possible to apply the HPTT process to longer samples. Samples were deformed by up to five turns of the die—again in an attempt to suppress non-homogeneity of strain in a cross-section of the tube similar to that found in HPT. The FE model of the process used is shown in Fig. 7, along with the evolution of the equivalent strain distribution in the sample with the degree of tool rotation calculated with the MARC software.

The equivalent strain in HPTT is given by [5]:

$$\varepsilon_{\text{eq}} = \frac{2\pi N \cdot R}{\sqrt{3} \cdot t}, \quad (3)$$

where  $N$  is the number of turns,  $R$  is the tube radius and  $t$  is the wall thickness.

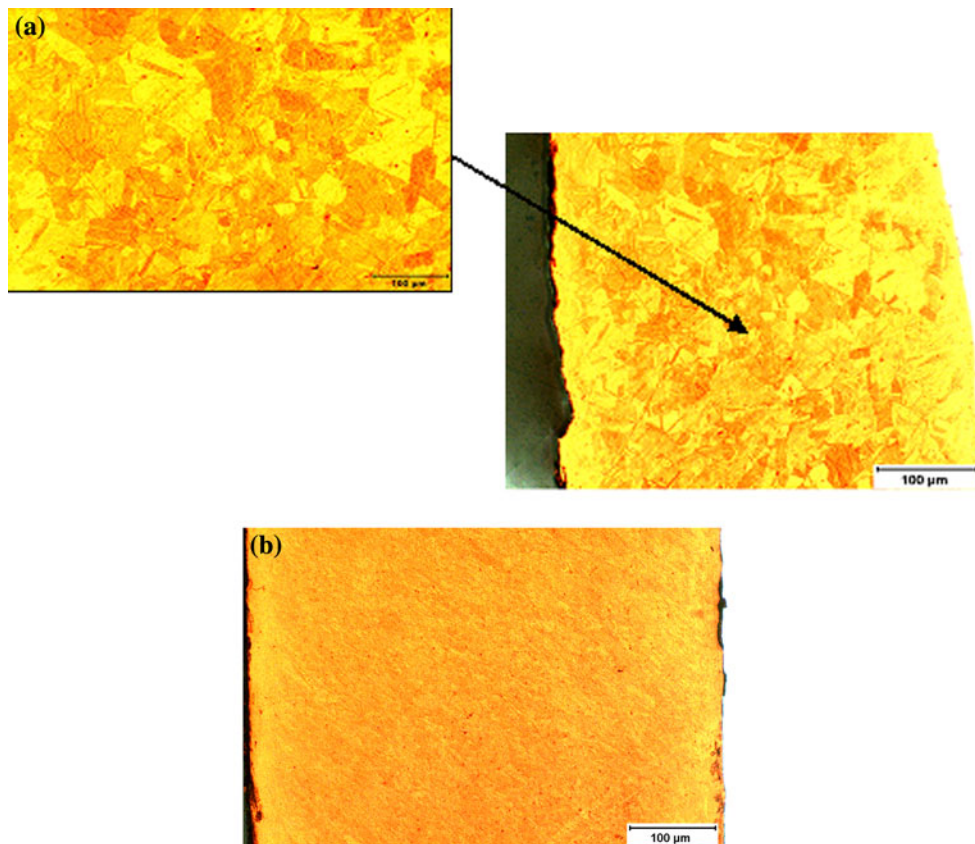
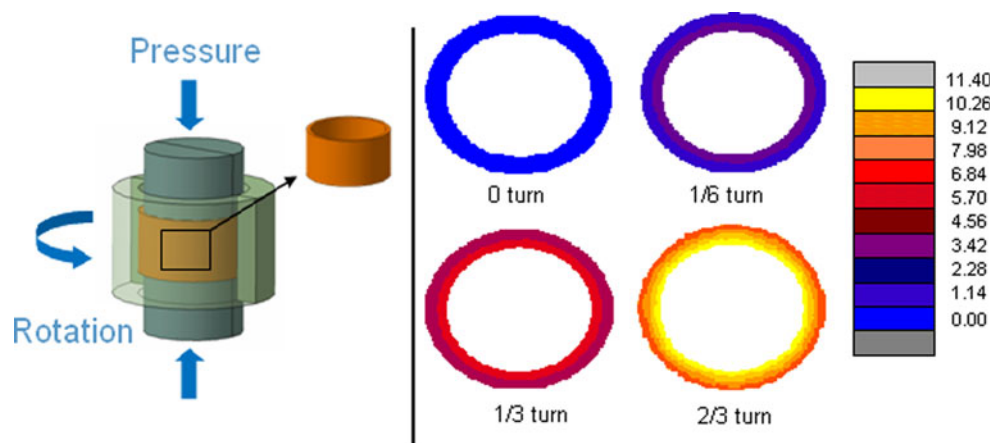


**Fig. 6** Microstructure of the cone-shaped specimen deformed by five turns of the punch **a** in the area close to the edge of the funnel; **b** in the middle section of the funnel normal to its axis

**Fig. 7** FE model of the HPTT process (*left*) and the evolution of the equivalent strain distribution in the sample with the degree of die rotation



An overall view of a vertical cut through a tube wall and its microstructure after HPTT are shown in Fig. 8. It can be seen that the thickness of the layer where the grains are refined substantially (below the OM resolution) is about one-third of the tube wall thickness, approximately 300  $\mu\text{m}$ .

Some slip between the tube and the die was observed during deformation causing non-uniformity of strain and microstructure within the wall thickness. In order to

confirm this and to estimate the grain size in both regions, SEM images were taken in a cross-section of the tube, Fig. 9. The uniform ultrafine grains less than 1  $\mu\text{m}$  in diameter, Fig. 9a, can be seen within a deformation zone of 300- $\mu\text{m}$  thickness with about 10- $\mu\text{m}$  thick layer of highly twisted grains. Close to the outer surface of the tube, the grain size was in the range of 10–40  $\mu\text{m}$ , which is consistent with some slip observed at the contact surface with the die.

**Fig. 8** Tubular sample deformed by five turns of HPTT  
**a** general view of a vertical section through a tube wall after deformation; and **b** OM image of the microstructure across the tube wall

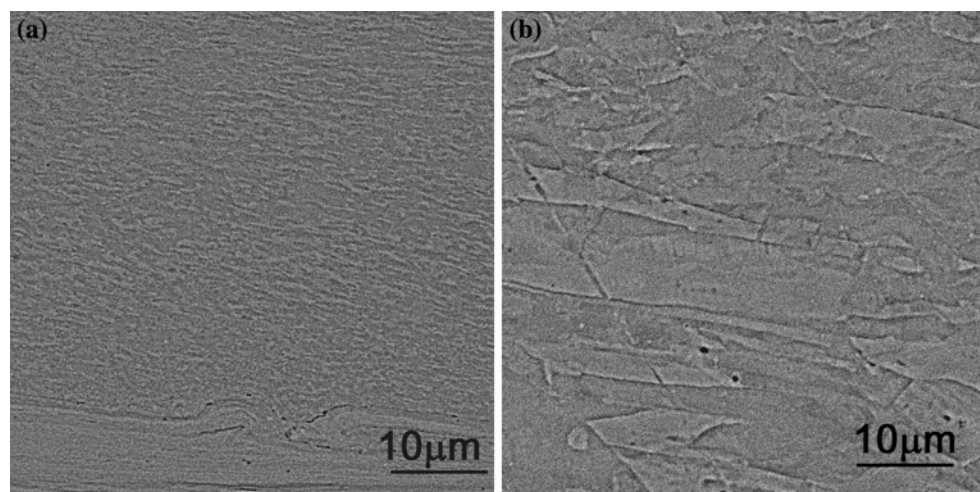
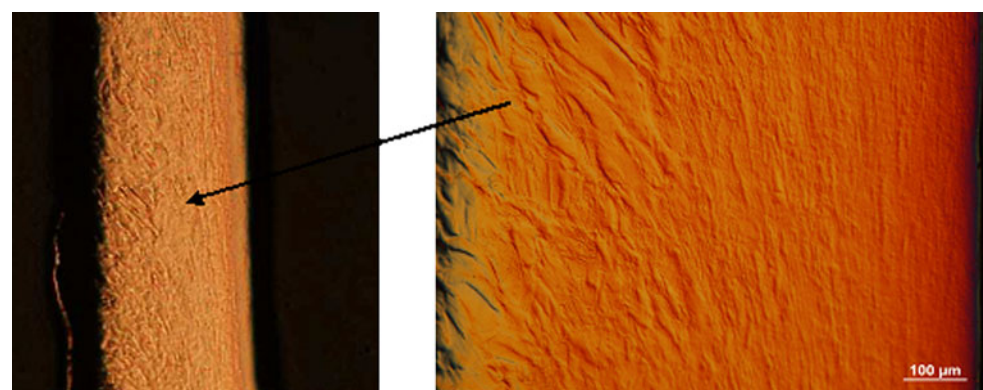


**Fig. 9** SEM images in a cross-section of a tube sample deformed by HPTT **a** area at the inner surface of the tube; **b** area close to the outer surface of the tube

A comparison of microstructure of copper samples deformed by all the three techniques, namely HPT, CCM and HPTT, with the microstructure of samples deformed by ECAP with back pressure shows that all the three thin samples have a non-uniform microstructure in the zones either close to the free surfaces or close to the contact surfaces. This is in contrast to the microstructure of ECAP samples, which is commonly reasonably homogeneous. The difference is associated with the absence of free surfaces during ECAP with back pressure as well as with different implementations of shear deformation. While in ECAP shear deformation is imposed by an abrupt change in the material flow direction, all the three processes discussed above rely on shear introduced through a relative velocity difference due to a friction force. Considering that friction forces in a contact pair depend on the contact micro-profile, non-uniform pressure, plastic deformation of asperities and possible local slip, uniformity of strain in the contact layer cannot be expected. The presence of small gaps or free surfaces in these processes resulting in partial extrusion of the sample also adds to the non-uniformity at

the sample (or work-piece) edges. In this study, the amount of slip was not evaluated quantitatively, but its ‘footprint’ can be clearly seen in the regions adjacent to the free surfaces where the strain was insufficient to cause grain refinement.

Despite the non-uniformity of strain in all the three processes discussed, it is believed that they have the potential of producing a uniform microstructure. Indeed, microstructure development under severe plastic deformation towards a refined grain size tends to saturate with strain. If the strain in the regions of a sample where the deformation is the smallest is sufficient for such saturation to occur, then the microstructure will be uniform regardless of how non-uniform the equivalent strain is [3, 4]. Of course, this does not apply to the regions of the sample where such levels of strain cannot be achieved by the very nature of the process (such as, e.g. the regions near the axis of an HPT specimen or near the free edge of a CCM specimen). However, even in those regions gradient effects may provide for development of more homogeneous microstructure [7]. By no means does the fact that the

desired degree of homogeneity has not been achieved in our first experiments with CCM and HPTT reported here indicate that this is not possible in principle.

## Conclusions

A particular group of SPD processes applicable to thin products—High Pressure Torsion, CCM and HPTT—were considered. These processes rely on shear applied by friction forces acting on the large surfaces and a high hydrostatic pressure within the deformation zone. All the three processes were applied to thin disc-shaped, conical or tubular samples made from commercially available pure copper with the grain size of 20 µm. The microstructures obtained experimentally, as well as the FE model predictions with regard to strain non-uniformity, were discussed. Through our experiments, it was demonstrated that the two new techniques, CCM and HPTT, can be realised in practice and do lead to microstructure refinement. However, despite the fact that these techniques are well-suited

for microforming of metals, uniform fine-grained microstructure is pretty difficult, although not impossible, to obtain. Further improvements of these processes leading to more uniform microstructures are under way.

**Acknowledgement** The help of Ms Wendy Borbridge with optical microscopy is gratefully acknowledged.

## References

1. Valiev RZ, Estrin Y, Horita Z, Langdon TG, Zehetbauer MJ, Zhu YT (2006) JOM 58(4):33
2. Zhilyaev AP, Nurislamova GV, Kim B-K, Baro MD, Szpunar JA, Langdon TG (2003) Acta Mater 51(3):753
3. Bouaziz O, Estrin Y, Kim HS (2007) Cahiers D'Inf Tech 104(6):318
4. Bouaziz O, Estrin Y, Kim HS (2009) Adv Eng Mater 11:982
5. Toth LS, Arzaghi M, Fundenberger JJ, Beausir B, Bouaziz O, Arruffat-Massion R (2009) Scripta Mater 60(3):175
6. Geiger M, Meßner A, Engel U (1997) Prod Eng 41:55
7. Estrin Y, Molotnikov A, Davies CHJ, Lapovok R (2008) J Mech Phys Solids 56(4):1186